Highly Hydrolysis-Resistant Polyimide Fibers Prepared by Thermal Crosslinking with Inherent Carboxyl Groups

Shi-Xu Zhou, Jie Dong, Xiu-Ting Li, Xin Zhao, and Qing-Hua Zhang[*]

State Key Laboratory for Modification of Chemical Fibres and Polymer Materials, College of Materials Science and Engineering, Donghua University, Shanghai 201620, China

Ⓔ Electronic Supplementary Information

Abstract Easy hydrolysis in alkaline environments limits the use of polyimide fibers in environmental protection. The hydrolysis resistance levels of polyimide fibers can be improved by crosslinking of the macromolecular chains. In this work, crosslinked polyimide fibers (CPI fibers) were produced by intrinsic carboxyl decarboxylation for the first time. The thermal stability of the polyimide fibers containing the intrinsic carboxyl groups (PIC fibers) was studied, and the temperature of the decarboxylation-crosslinking reaction was determined to be 450 °C. The PIC fibers were hot-drawn to initiate thermal crosslinking of the carboxyl groups and molecular chain orientation at high temperature. The CPI fibers had high tensile strengths (0.72–1.46 GPa) and compressive strengths (401–604 MPa). The oriented macromolecules and chemically crosslinked structure improved the tightness of the molecular chains and endowed the CPI fibers with excellent hydrolytic resistance. The CPI-50 fiber did not dissolve in a 0.5 wt% NaOH solution during heating at 90 °C for 10 h, and the tensile strength retention reached 87% when treated in 0.5 wt% NaOH solutions at 90 °C for 1 h, providing a guarantee for its application in alkaline corrosive environments.

Keywords Polyimide; Carboxyl group; Crosslinking; Hydrolysis-resistance

INTRODUCTION

Air pollution has become a major environmental concern due to the large amount of air pollutants emitted from industrial facilities such as chemical plants and power plants. Generally, high-temperature industrial flue gases must be filtered with high-performance textiles to remove particulate matter.[1] Polyimide (PI) fibers are known to have excellent properties, such as high mechanical performance, high temperature resistance, corrosion resistance, radiation resistance, flame retardancy, and nontoxicity.[2–6] Therefore, PI fibers are an important high-temperature filter material, and filter bags made by PI fibers can meet the basic requirements for industrial flue gas filtration.[7–9] The high-temperature flue gases emitted by industry generally contain sulfur oxide, nitrogen oxides or alkaline gases. These chemical substances easily catalyze the decomposition of the PI filter, which reduces the dust removal performance and decreases the filtration efficiency.[10,11] Therefore, polyimide has good corrosion resistance, which is important for ensuring the long-term stable operation of dust removal equipment.

However, polyimides are unstable to hydrolysis caused by the structure of anhydride, especially under heating and alkaline conditions.[12] The alkaline hydrolysis of PI involves the attack of OH⁻ on the carbonyl carbon of imide ring to form an unstable monoanion adduct by nucleophilic addition and decomposition of the intermediate to the carboxylate salt, which causes breaking of the macromolecular chain and a decrease in performance.[13] This hydrolysis tendency is related to the structure of the monomers from which the polyimide is synthesized. The greater the activity of the dianhydride, the easier the polyimide hydrolysis. The introduction of crosslinking into the PI material is a preferred way to keep the alkali solutions from corroding the PI fibers. This increases the interactions between the molecular chains and slows the erosion process, thereby improving the alkali resistance throughout the fiber.[14–16]

Various approaches have been used to build crosslinked structures inside polyimide materials. Chemical crosslinking of polyimides *via* covalent bonds provides excellent resistance to many organic solvents due to the rigid structure in the polymer backbone. Toh *et al.* used 1,6-hexamethylenediamine to crosslink a P84 polyimide produced by Evonik Industries and prepared nanofiltration membranes resistant to organic solvents.[17] The results demonstrated that the crosslinked structure enhanced the solvent resistance by preventing solvent intrusion into the membranes. Park *et al.* synthesized crosslinked sulfonated polyimides with various gly-

cols with different chain lengths to control the water uptake and proton conductivity of the membranes and found that excessive crosslinker chain lengths reduced the strength and solvent resistance of the material.[18]

Nevertheless, small-molecule chemical crosslinkers have several shortcomings that cannot be ignored. The thermal performance of the polyimide will be significantly reduced if the aliphatic segments in small-molecule crosslinkers decompose and break easily at high temperature.[17,19] The thermal crosslinking method is more suitable for PI filter materials that form network structures, since it directly crosslinks aromatic rings without introducing aliphatic chains. The mechanism involves aromatic ring dehydrogenation and produces free radicals, and intermolecular crosslinks are produced when they are coupled.[20] In fact, all aromatic heterocyclic polymers can be crosslinked by generating free radicals at high temperature (above 550 °C), but these process is usually accompanied by decomposition of the polymer, even with a PI material.

Previous studies have shown that polyimides with carboxyl groups formed crosslinks at temperatures below the decomposition temperatures *via* thermal decarboxylation. Kratochvil *et al.* suggested a novel crosslinking method for a carboxylic acid-containing polyimide.[21] The polyimide generated free radicals by decarboxylating the carboxyl groups at 405 °C, and these radicals attacked other portions of the polyimide for crosslinking. Qiu *et al.* used 3,5-diaminobenzoic acid to synthesize a kind of polyimide containing side-chain carboxyl groups.[22] Additionally, thermal crosslinking of this polyimide occurred at a low temperature even below the glass transition temperature. Crosslinking of the polyimide by thermal decarboxylation avoided degradation of the polyimide at excessively high temperatures.

In fact, thermal decarboxylation crosslinking is quite suitable for introducing crosslinked structures into PI fibers. The PI fibers need to be drawn at high temperatures above T_g to achieve molecular chain orientation. The thermal decarboxylation reaction temperatures (350–450 °C) confirmed in the above studies were consistent with the thermal drawing temperatures of the PI fibers.[21–24] Therefore, for carboxyl acid-

containing PI fibers, thermal decarboxylation and orientation of the molecular chain can occur simultaneously during the hot drawing process.

To obtain polyimide fibers with crosslinked structures, polyimide fibers containing inherent carboxyl groups (PIC fiber) were developed in this work. After hot drawing at a temperature between 380–450 °C in the fiber processing, the fibers developed crosslinked structures and oriented molecular chains. The process for thermal crosslinking of the fibers was characterized by thermal analysis, and the hydrolytic resistance of the crosslinked fibers was determined.

EXPERIMENTAL

Materials

3,3',4,4'-Biphenyltetracarboxylic dianhydride (BPDA) and *N,N*-dimethylacetamide (DMAc) were obtained from Zhengzhou Alpha company, and the BPDA was purified in a vacuum oven at 190 °C for 24 h before use. 4,4'-Oxydianiline (ODA), 3,5-diaminobenzoic acid (DABA), *m*-phenylenediamine (mPDA) and NaOH (AR) were purchased from TCI.

Synthesis of Polyimide Fibers

PIC fibers were synthesized by copolymerization, and the chemical structure is shown in Fig. 1(a). The DABA monomer has a pendent carboxyl group in the chemical structure, so PIC fibers with different carboxyl contents were obtained by adjusting the proportion of DABA monomer. PIC fibers with DABA molar ratios in diamines of 0 mol%–50 mol% were prepared, and these are referred to as PIC-*x*, where *x* represents the proportion of DABA monomer.

Taking the PIC-50 fibers as an example, the typical preparation method was as follows: DABA (3.32 g, 21.9 mmol), ODA (4.37 g, 21.9 mmol), and DMAc (150 mL) were added to a three-neck flask. The solution was stirred at room temperature for 1 h to dissolve the diamine, and BPDA (12.86 g, 43.8 mmol) was added into the flask in two portions. The solution was stirred at room temperature under N_2 for another 24 h to form a viscous and homogeneous poly(amic acid) (PAA-50) solution. The PAA-50 solution was used as the spinning dope
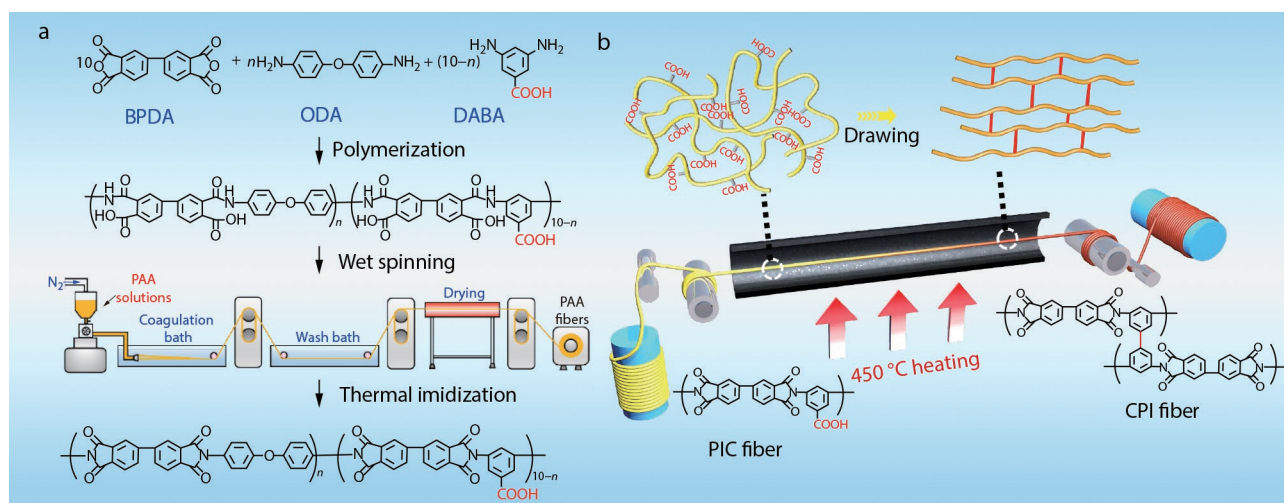

Fig. 1 (a) Synthetic route to the PIC fibers; (b) Hot drawing process and the initiation of the crosslinking reaction of PIC fibers.

to prepare fibers by wet spinning after defoaming. The PAA-50 fibers were heated in a vacuum oven at 100, 200 and 300 °C for 1 h. In this process, the fibers were completely converted to the imide structure. PIC-50 fibers were finally obtained after hot drawing at 320 °C.

mPI-50 fibers without carboxyl groups were prepared as a comparison sample of PIC-50, using the same method but with mPDA instead of DABA in the copolymerization.

Thermal Crosslinking of the PIC Fibers

Crosslinked polyimide fibers (CPI fibers) were obtained by further hot drawing of the PIC fibers at 450 °C. In the process of drawing, the orientations of the macromolecular chains and crosslinking initiated by the carboxyl groups occurred simultaneously. For each PIC fibers, an effort was made to achieve the maximum drawing ratio.

Hydrolysis-resistance Test

CPI fibers (0.2 g) was placed in a nonwoven bag, soaked in 0.5 wt% NaOH aqueous solution at 90 °C for 1 h, and then removed. After washing and drying, the mechanical properties of the fibers were tested. The mechanical properties were compared with those of untreated fibers to calculate the retention rate. This hydrolysis treatment condition can quantitatively evaluate the alkali resistance of all samples in present work and is widely used.

CPI-0, CPI-50 and mPI-50 (hot drawn at 450 °C) fibers were placed in a sample bottle with 0.5 wt% NaOH solution, and the bottle was placed in a 90 °C water bath. The bottles were taken out at regular intervals to observe and record the fiber status.

Characterizations

^{1}H-NMR spectra of the PAA were collected with a nuclear magnetic resonance spectrometer (NMR, Bruker Avance). The structural transitions and hydrogen bonding interaction were studied with Fourier transform infrared spectroscopy (FTIR, Nicolet 8700). The morphologies of the fibers were observed by SEM (HITACHI SU8010). The inherent viscosities of the PAA solutions were measured with an Ubbelok viscometer. The dynamic mechanical properties of fibers were tested by DMA (TA Q800) with temperature increases of 5 °C/min under N_2. The thermal properties were tested by TGA (Netzsch 209F3) with temperature increases of 10 °C/min under N_2. TGA-IR and TGA-MS were used to analyze the vapors released from the PIC-50 fibers during heating. The molecular weights of the released gases were obtained with a Thermostar GSD-320 mass spectrometer (MS, Thermostar GSD-320). Structures of the released gases were determined by FTIR (Bruker Tensor 27). Mechanical properties of the fibers were obtained with a tensile testing instrument (Xinxian XQ-1) with a drawing rate of 10 mm/min and a gauge length of 20 mm. The compressive strengths of the CPI fibers were measured with a single fiber tensile-recoil test, and the critical value for fiber compressive failure was considered the compressive strength.[25] X-ray photoelectron spectroscopy (XPS) was carried out with an Escalab 250Xi System using a monochromatic Al X-ray source (987.9 W, 1486.6 eV). The XRD pattern of fibers were obtained with an X-ray diffractometer (D/max 2550VB/PC). The orientation of fibers was calculated by Hermans' orientation factor.[26]

RESULTS AND DISCUSSION

Structural Characterization of the PIC Fibers

Fig. 2(a) shows the ^{1}H-NMR spectra of PAAs (precursors of PIC) with DABA mole ratios ranging from 0 mol% to 50 mol%, which corresponds to the PICs with different contents of carboxyl groups. The diamine ratios in the copolymers were verified easily by the H signals at 10.47 and 10.72 ppm, which were attributed to amide groups connected with the ODA structure and DABA structure, respectively. In addition, the PAA samples exhibited a broad peak at approximately 13.20 ppm attributed to the carboxyl groups of the polyamic acid structure and DABA moiety. The peak distribution within the range of 6.5–9.0 ppm for PAA-50 were very consistent with the proposed molecular structure, indicating that the predetermined PAA structure was successfully synthesized.

The carboxyl group and two amine groups of the DABA monomer were distributed in the meta positions of the benzene rings. The electron with drawing effects of the carboxyl groups reduces the reactivity of the amine groups to a certain extent, so the inherent viscosity of the PAA solutions (Fig. 2b) decreases with increasing DABA content. Nevertheless, the viscosities of the synthesized PAA solutions ranged from 1.54–3.02 dL/g, which make sure that all PAA solutions can be successfully utilized to prepare PAA precursor fibers by wet spinning. The prepared PAA fibers had uniform and complete morphologies (Fig. 2d). After thermal imidization, the characteristic absorption band for the amide groups in the PAA fibers (1543 and 1660 cm^{-1}) completely disappeared, and a series of absorption bands for imide structures appeared in the FTIR spectra of PIC (Fig. 2c). PIC-50 shows a weak dispersion band at 2900–3300 cm^{-1}, which may have been caused by the inherent carboxyl groups in the DABA structure.

The hydrogen bonds formed between the carboxyl groups and the polar groups caused the absorption band to shift to a lower energy.[27] As shown in Figs. 2(e) and 2(f), the FTIR spectra of PIC-50 and mPI-50 were measured during *in situ* heating from 30 °C to 240 °C. With the increasing temperature, the absorption bands for the C—N—C stretching in imide ring (1348–1367 cm^{-1}) and the ether bond (1236 cm^{-1}) shifted to higher wavenumbers. However, the controlled mPI-50 sample did not show this phenomenon. It is suggested that the hydrogen bonds formed between the carboxyl groups and polar groups (Fig. 2g) were destroyed during *in situ* heating, and this caused shifts to higher wavenumbers for the vibrational signals of the polar groups. The hydrogen bonds indirectly proved that the prepared PIC fibers containing abundant carboxyl groups.

Thermal Crosslinking of the PIC Fibers

Since the thermal crosslinking temperatures of the PIC fibers are closely related to the main chain structures in which the pendent carboxyl groups are located, the crosslinking temperature of the PIC fibers must be determined first by thermal analysis. TGA and DMA tests were conducted on PIC-0, PIC-10, PIC-30 and PIC-50 fibers as representatives to analyze the thermal properties of PIC fibers.

The weight-loss curves of the PIC fibers during heating showed three weight-loss events, which were sequentially
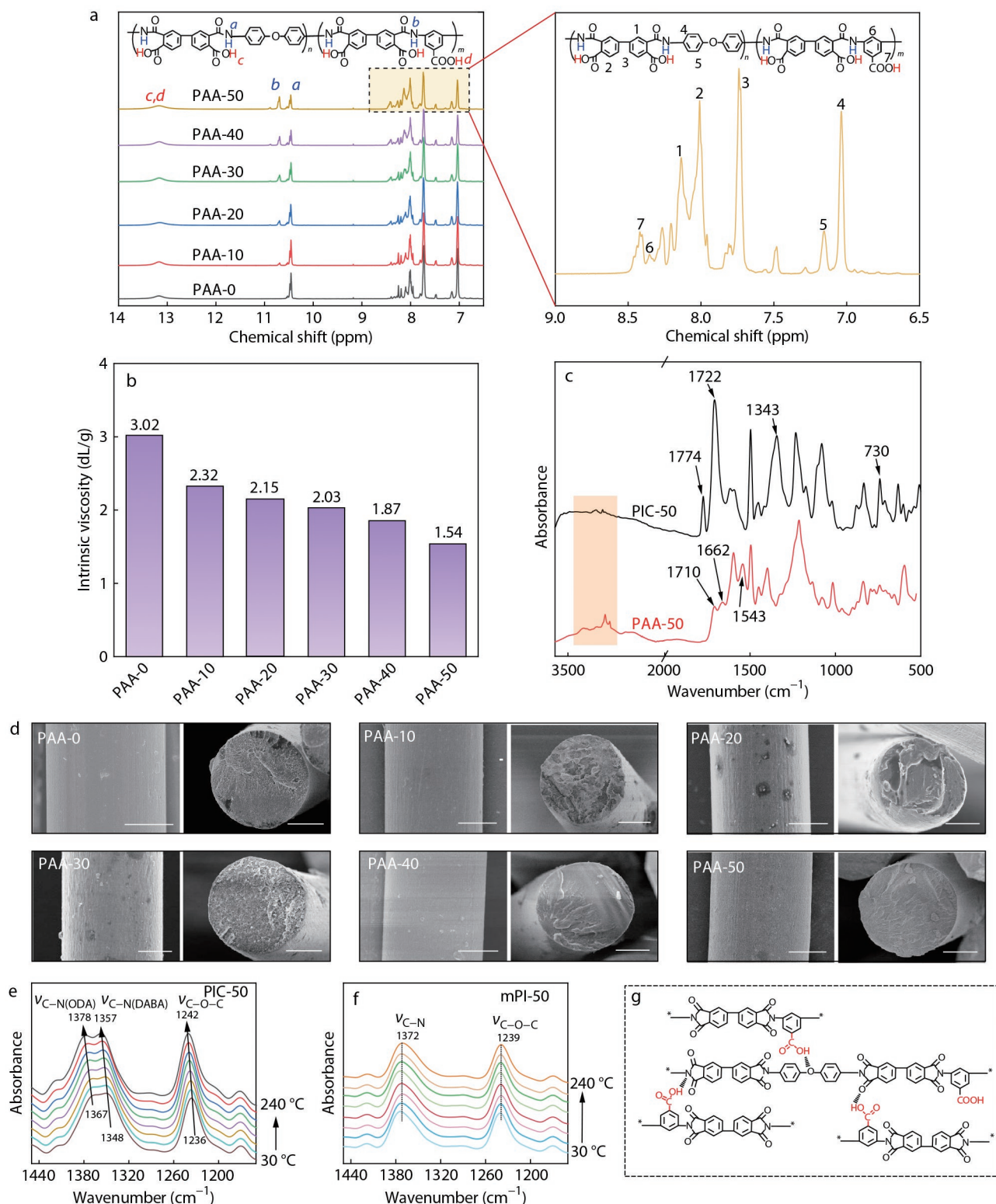
Fig. 2 (a) ^{1}H-NMR spectra of PAAs with different DABA molar ratios; (b) Inherent viscosities of the PAA solutions used for wet spinning; (c) FTIR spectra of PAA-50 and PIC-50; (d) Surface and cross-section morphologies of the PAA fibers, and the white strips represent 10 μm; *In situ* FTIR spectra of (e) PIC-50 and (f) mPI-50 fibers as heated from 30 °C to 240 °C; (g) Schematic illustration of hydrogen bonds in the PIC fibers.

caused by residual solvent removal, decarboxylation and macromolecular chain decomposition (Fig. 3a). The crosslinking reaction initiated by decarboxylation occurred at 400–

500 °C, so the weight loss of the PIC fibers was significantly increased within this temperature range. The thermal weight loss of PIC-50 at 500 °C was 5.4%, which was significantly
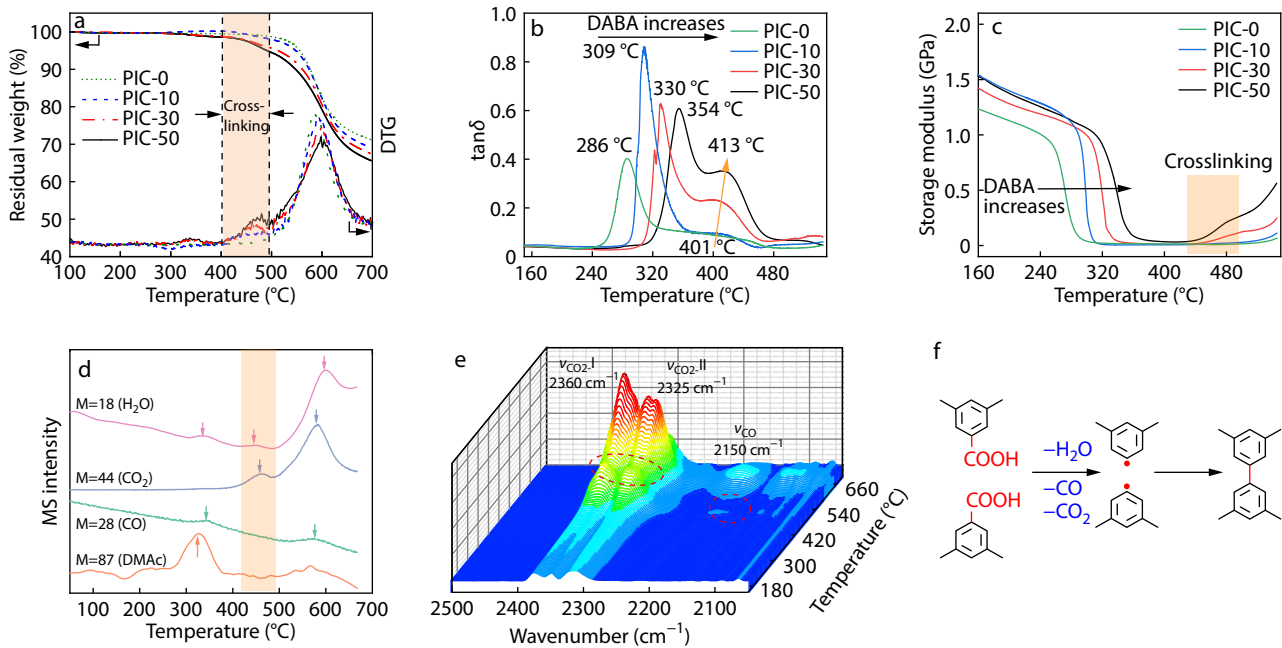
Fig. 3 (a) TGA and DTG curves of the PIC fibers; (b, c) tanδ curves and storage modulus of the PIC fibers in the DMA tests; (d) MS signals for the gases release from PIC-50 during the TGA test with m/z=18, 28, 44 and 87; (e) 3D TGA-IR analyses of PIC-50; (f) The crosslinking process between the pendent carboxyl groups.

higher than that of the PI-0 (1.3%). However, crosslinking increased the thermal stability of the main chains, so the maximum thermal decomposition temperature of the PIC-50 fibers was 17 °C higher than that of PIC-0.

Fig. 3(b) shows the tanδ curves of the PIC fibers with different carboxyl group contents. The obvious relaxation process occurring between 286 and 354 °C was caused by the glass transition (T_g) of the PIC fibers. T_g increased as the DABA content increased due to the more rigid structure of the DABA monomer in comparison to ODA. Another distinct T_g appeared in the PIC-30 and PIC-50 curves at approximately 410 °C. In fact, the carboxyl group can also be removed at lower temperatures to initiate crosslinking, although the reaction progresses slowly.[22] It is believed that a small amount of cross-linked structures were formed prior to reaching 400 °C during DMA testing. These cross-linked structures exhibited a higher glass transition temperature than the uncrosslinked portions, resulting in significant shoulder peaks in the PIC fibers. In Fig. 3(c), it is noteworthy that the storage modulus of PIC-50 fibers with carboxyl groups showed an obvious increase after being heated to 440 °C compared to the PIC-0, which was lower than its carbonization temperature. Therefore, it is believed that the increase in the storage modulus of PIC at this temperature is due to the formation of cross-linked structures through thermal decarboxylation reaction.

The mechanism for PIC crosslinking initiated by the intrinsic carboxyl groups (Fig. 3f) involves the decomposition of carboxyl group under high temperatures to form free radicals, and then free radical coupling results in a direct chemical bond between the two benzene rings.[28,29] This process was confirmed with the small molecules (CO_2, CO and H_2O) release produced by carboxyl removal. Fig. 3(d) shows the MS spectrum obtained during thermal decomposition of the PIC-

50 fibers. The signals for water and CO_2 (m/z=18 and 44) showed signal peaks within the crosslinking reaction near 450 °C, which obviously differed from the peaks for solvent removal and macromolecular chain decomposition. The temperature for water loss was slightly lower than that for CO_2, which was related to the fact that the two carboxyl groups first dehydrated to form an anhydride before producing the free radicals. Due to the nitrogen purge used during the tests, the contribution of CO on the strength of the m/z=28 signal was not obvious. However, the TGA-IR test (Fig. 3e) confirmed that some CO released during the reaction, but its content was far lower than that of CO_2. Fig. S1 (in the electronic supplementary information, ESI) shows the variation of the absorption intensity at 2325 cm^{-1} (representing CO_2) during TGA-IR test. In short, the PIC fibers completed the crosslinking reaction by releasing water and CO_2 at 400−500 °C.

Mechanical Properties of the PIC and CPI Fibers

Thermal analysis revealed that the temperature range for crosslinking reaction was between 400−500 °C. Therefore, we chose 450 °C as the post hot drawing treatment temperature for the PIC fibers, as this temperature can induce thermal crosslinking without triggering the decomposition of macromolecular chains. During the heat treatment, the orientation of PIC macromolecular chains and crosslinking reaction occur simultaneously.

The tensile strength of PIC fibers ranges from 0.5 GPa to 1.1 GPa, with an elongation at break of 20.6%−27.1% (Fig. 4a and Table S2 in ESI). When DABA participates in the copolymerization reaction, it disrupts the ordered arrangement of molecular chains in the PIC fibers, thereby reducing their crystallinity and causing the elongation at break of the fibers to increase with increasing content of DABA monomer. Additionally, it could be observed that the strength of fibers also decreases.
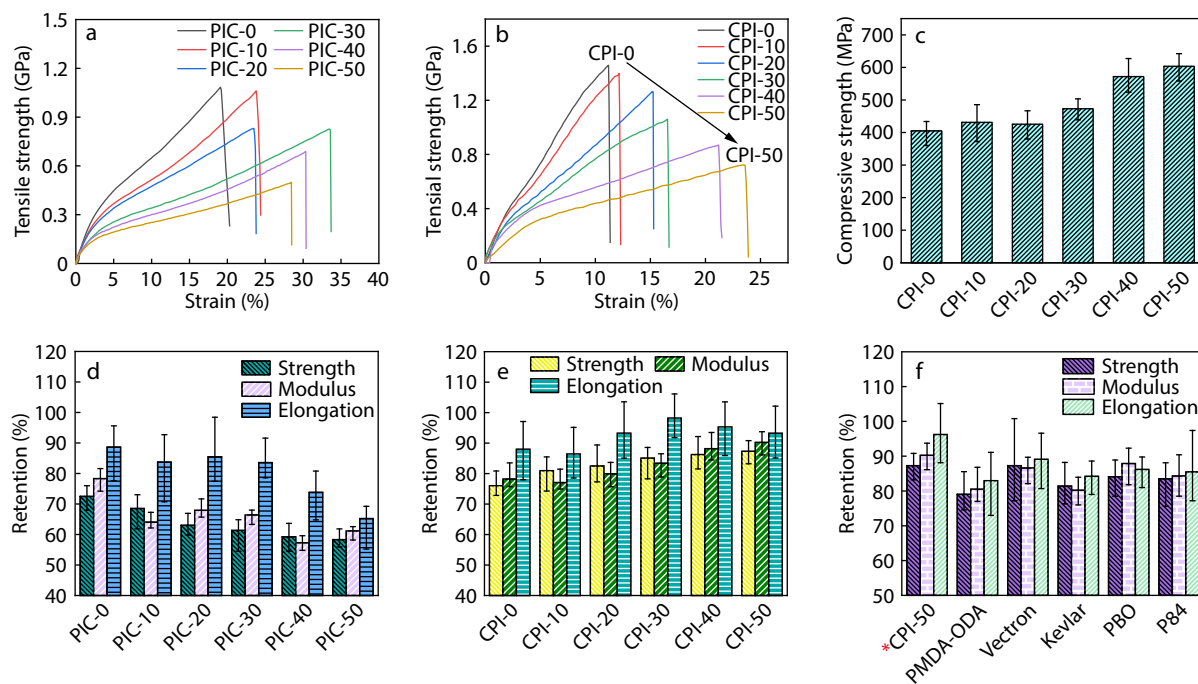
Fig. 4 Typical tensile curves for (a) PIC fibers and (b) CPI fibers; (c) Axial compressive strengths of the CPI fibers; Retention rates for the mechanical properties of (d) PIC fibers and (e) CPI fibers after hydrolysis for 1 h; (f) Comparison of the mechanical retention between CPI-50 and other commercial fibers after hydrolysis for 1 h.

The twisted molecular chain caused by the inter-phenyl structure of DABA affects the fiber performance.[30] Furthermore, the lower reactivity of DABA monomer compared to ODA results in a decrease in the intrinsic viscosity of the synthesized PAA precursor (Fig. 2b).

Comparatively, the mechanical properties of the CPI fibers were significantly improved after hot drawing at 450 °C, with the tensile strengths ranging from 0.72 GPa to 1.46 GPa (Fig. 4b and Table S2 in ESI). The improvement in tensile properties may be mainly attributed to the enhancement of molecular chain orientation by hot drawing. Generally, gaseous substances, coming from the residual solvents and by-products during the fabrication process, may form some macro- or micropores in the fibers, and it is a common phenomenon especially in the wet-spun fibers, such as the carbon fiber, cellulose fiber, etc. The cross-section morphology of the CPI-50 fiber is dense and uniform as depicted in Fig. S2 (in ESI). The tension generated by the hot drawing can effectively counteract the infect of escaped gas molecules and make the fiber's structure dense.

As illustrated in Fig. 4(c), the compressive strength of CPI fibers ranges from 405–604 MPa, with CPI-50 exhibiting a 51% higher compressive strength than the CPI-0. This is because the CPI-50 contains more cross-linking structures, which increase the intermolecular interactions between molecular chains, thereby enhancing the fiber's cohesion and compressive performance.[25]

Hydrolysis Resistance of the CPI Fibers

Polyimide materials are known to be easily susceptible to hydrolysis, particularly in alkaline environments. The formation of crosslinked structures within the materials can enhance their resistance to hydrolysis by limiting the entry of solvent into the

material.[31,32] To evaluate the improvement in hydrolytic resistance resulting from thermal crosslinking, both PIC and CPI fibers were immersed in 0.5 wt% NaOH solutions at 90 °C for 1 h to evaluate their mechanical retentions.

As shown in Fig. 4(d), after hydrolysis, the strength of PIC fibers decreased significantly. The strength retention rate of PIC-0 fiber was 72%, while that of PIC-50 was only 58%. This can be attributed to the enhanced hydrophilicity of the fibers due to the presence of polar carboxyl groups, which resulted in a significant decrease in strength of the PIC-50 fibers. After hot drawing, the hydrolysis resistance of CPI fibers was greatly improved, especially for CPI-50 with a strength retention of 87% (Fig. 4e). The strength retention of CPI fibers increased with increasing DABA content, indicating that carboxyl removal and crosslinking structure formation enhanced the hydrolysis resistance of the fibers. The retention rate of CPI-0 also increased from 72% to 76%, which may be related to the improvement of molecular packing structure. In Fig. 4(f), other commercial high-performance fibers were also exposed to the same hydrolysis treatment as the CPI-50 fibers for comparison. Clearly, the CPI-50 demonstrated an excellent resistance to hydrolysis in of alkaline solutions.

PIC-50, mPI-50 (hot drawn at 450 °C), and CPI-50 fibers were immersed in alkaline solution to compare their hydrolysis resistances. As shown in the Fig. 5(a), these three fibers represent different molecular chain and aggregate structures: PIC-50 fibers have a non-crosslinked and low-orientation degree molecular chain structure, the hot-drawn mPI-50 fibers have a higher oriented structure, and CPI-50 fibers have a crosslinked and oriented structure. The PIC-50 fibers clearly collapsed after 5 h and were completely dissolved after 13 h in the alkaline solution. The mPI-50 fibers curdled into a mass after 10 h
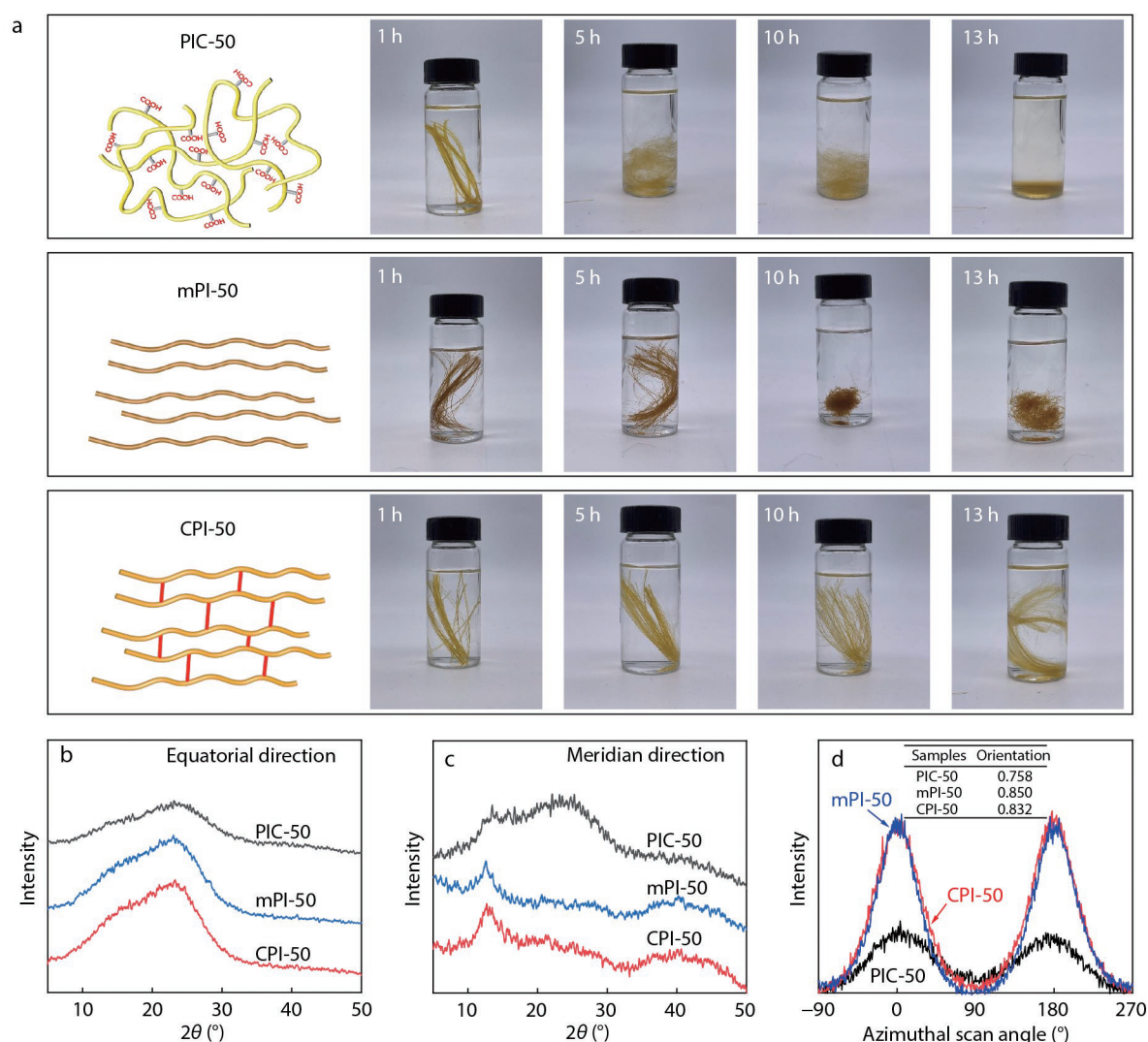
Fig. 5 (a) Digital photos of PIC-50, mPI-50 and CPI-50 fibers immersed in 0.5 wt% NaOH solution at 90 °C with different time; (b, c) XRD patterns of PIC-50, mPI-50 and CPI-50 fibers in the equatorial and meridian directions; (d) Azimuthal scans (at $2\theta=12.8°$) and corresponding orientations of the PIC-50, mPI-50 and CPI-50 fibers.

and swelled obviously after 13 h. The CPI-50 fibers had a tendency to collapse after soaking for 13 h, but they remained in a stretched state. The PIC-50 fibers collapsed quickly in the alkaline solution because the intrinsic carboxyl groups easily forming anions in the NaOH solution, which increased the hydrophilicity of the fibers and accelerated the penetration of the NaOH solution into the fibers. The orientation of the macromolecular chains in mPI-50 fibers made the aggregated structure denser, which also improved the hydrolytic resistance of fibers. Compared with the mPI-50, the CPI-50 fibers showed a better hydrolytic resistance. Obviously, the improvement in the CPI-50 sample was mainly attributed to the formation of a crosslinked structure. To demonstrate the degree of fibers orientation, XRD patterns of the PIC-50, mPI-50 and CPI-50 fibers obtained in the equatorial and meridian directions are presented in Figs. 5(b) and 5(c). The crystallinity and signal intensity of the PIC-50 fibers are lower compared to those of the mPI-50 and CPI-50 fibers. Fig. 5(d) shows the azimuthal scans at $2\theta=13.6°$ and orientation factor of these

fibers. The PIC-50 fibers exhibited the lowest orientation factor with 0.76. The orientation factor of the CPI-50 fibers was 0.83, slightly lower than that of the mPI-50 fibers with 0.85, which might have been affected by the crosslinking structure formed during the hot drawing process.

SEM images of the three types of fibers after 1 h of hydrolysis are presented in Fig. 6(a). The PIC-50 fibers exhibited a rough surface topography with numerous grooves and ravines, while the surface of mPI-50 fibers was smoother with fewer signs of alkaline hydrolysis. The CPI-50 fibers, which was crosslinked by hot drawing at 450 °C, showed a smooth and complete surface morphology, indicating the least effect of hydrolysis.

Element contents of the fibers surfaces before and after hydrolysis are presented in Table S4 (in ESI). The content of oxygen in crosslinked CPI-50 fibers increased slightly after hydrolysis, whereas that of PIC-50 increased by 5.6%. Hydrolysis of the imide rings in PIC fibers caused an increase in oxygen content. The O1s XPS spectra can further confirm the hydroly-
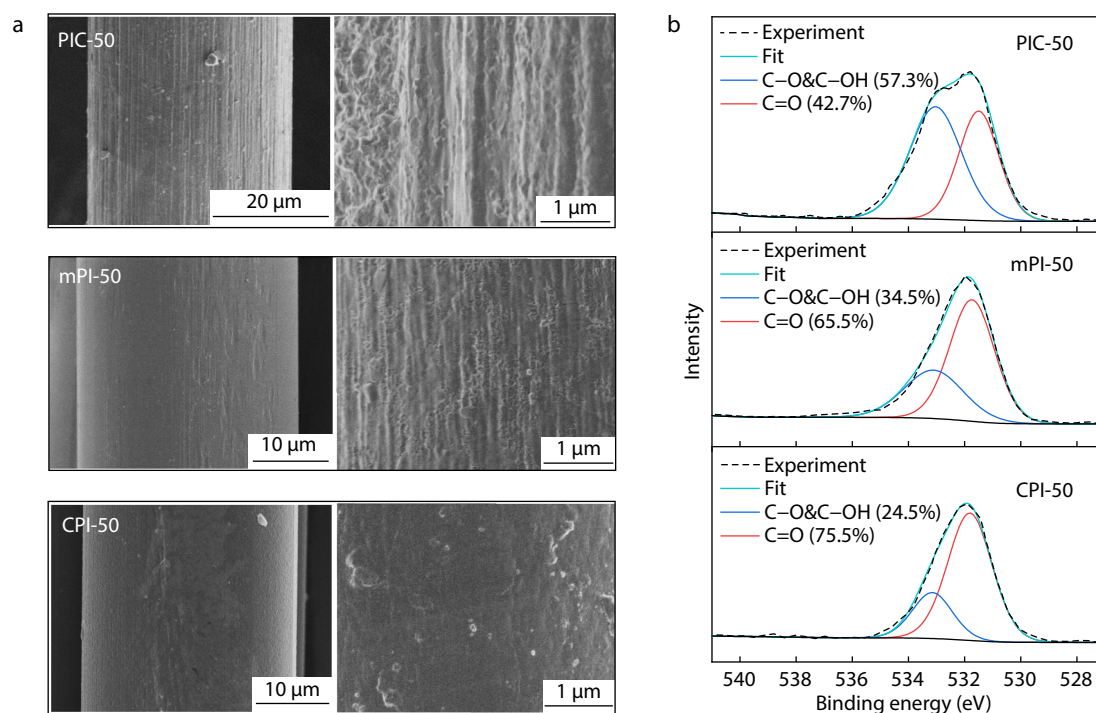
Fig. 6 (a) Surface morphologies and (b) O 1s XPS spectra of the PIC-50, mPI-50 and CPI-50 fibers after hydrolysis for 1 h.

sis degree of the fibers. In Fig. 6(b), the O1s XPS spectrum of the hydrolyzed fibers shows two peaks at 531.6 and 533.1 eV.[33] The low binding energy peak (pink line) attributes to the carbonyl double-bonded oxygen in the carboxyl and amide groups. The high binding energy peak (blue line) attributes to the hydroxyl oxygen in the carboxyl groups and the single-bonded oxygen in the ether linkages. The content of ether bonds in the three types of fibers is relatively constant and low. Therefore, the peak area of sing-bonded oxygen at 533.1 eV can reflect the amount of carboxyl groups generated by hydrolysis. The peak area at 533.1 eV of PIC-50 reached 57.3%, verifying the high degree of hydrolysis in PIC-50 fibers. The peak area at 533.1 eV of CPI-50 was 24.5%, which was lower than the 34.5% ratio for mPI-50 fibers, indicating that the CPI fibers with the crosslinked structures had stronger hydrolysis resistance.

CONCLUSIONS

PIC fibers with various DABA contents were prepared by wet spinning and copolymerized with carboxyl groups. Thermal analyses showed that the carboxyl groups underwent thermal decarboxylation and crosslinking reactions under 400–500 °C, accompanied by the release of small molecules. Based on reaction rates and material degradation, a thermal drafting temperature of 450 °C was found to be optimal for the PIC fibers. CPI fibers obtained by thermal drawing have good mechanical properties, with a tensile strength ranging from 0.72 GPa to 1.46 GPa. The crosslinked structure significantly improves the compressive strength of the fibers, with CPI-50 reaching 603 MPa. Moreover, the crosslinked and highly oriented structures produced by thermal drawing greatly enhanced the fibers' hydrolytic resistance, extending their service life.

Conflict of Interests

The authors declare no interest conflict.

Ⓔ **Electronic Supplementary Information**

Electronic supplementary information (ESI) is available free of charge in the online version of this article at http://doi.org/10.1007/s10118-023-3015-2.

REFERENCES

1 Mukhopadhyay, A.; Pandit, V.; Dhawan, K. Effect of high temperature on the performance of filter fabric. *J. Ind. Text.* **2015**, *45*, 1587−1602.

2 Liaw, D. J.; Wang, K. L.; Huang, Y. C.; Lee, K. R.; Lai, J. Y.; Ha, C. S. Advanced polyimide materials: syntheses, physical properties and applications. *Prog. Polym. Sci.* **2012**, *37*, 907−974.

3 Zhou, Z. X.; Zhang, Y.; Liu, S. W.; Chi, Z. G.; Chen, X. D.; Xu, J. R. Flexible and highly fluorescent aromatic polyimide: design, synthesis, properties, and mechanism. *J. Mater. Chem. C* **2016**, *4*, 10509−10517.

4 Rusu, R. D.; Constantin, C. P.; Drobota, M.; Gradinaru, L. M.; Butnaru, M.; Pislaru, M. Polyimide films tailored by UV irradiation: surface evaluation and structure-properties relationship. *Polym. Degrad. Stabil.* **2020**, *177*, 109182−109294.

5   Liu, H.; Chen, X. Y.; Zheng, Y. J.; Zhang, D. B.; Zhao, Y.; Wang, C. F.; Pan, C. F.; Liu, C. T.; Shen, C. Y. Lightweight, superelastic, and hydrophobic polyimide nanofiber /MXene composite aerogel for wearable piezoresistive sensor and oil/water separation applications. *Adv. Funct. Mater.* **2021**, *31*, 2008006−2008017.

6   Mai, A. T. M.; Thakur, A.; Ton, N. N. T.; Nguyen, T. N.; Kaneko, T.; Taniike, T. Photodegradation of a semi-aromatic bio-derived polyimide. *Polym. Degrad. Stabil.* **2021**, *184*, 109472−109478.

7   Chang, Y. S.; Kumari, P.; Munro, C. J.; Szekely, G.; Vega, L. F.; Nunes, S.; Dumee, L. F. Plasticization mitigation strategies for gas and liquid filtration membranes-a review. *J. Membr. Sci.* **2023**, *666*, 121125−121150.

8   Zhang, R. F.; Liu, C.; Hsu, P. C.; Zhang, C. F.; Liu, N.; Zhang, J. S.; Lee, H. R.; Lu, Y. Y.; Qiu, Y. C.; Chu, S.; Cui, Y. Nanofiber air filters with high-temperature stability for efficient PM2.5 removal from the pollution sources. *Nano Lett.* **2016**, *16*, 3642−3649.

9   Xie, F.; Wang, Y. F.; Zhuo, L. H.; Ning, D. D.; Yan, N.; Li, J. Y.; Chen, S. S.; Lu, Z. Q. Multiple hydrogen bonding self-assembly tailored electrospun polyimide hybrid filter for efficient air pollution control. *J. Hazard. Mater.* **2021**, *412*, 125260−125260.

10 Wang, L.; Cui, L.; Liu, Y.; Riedel, J.; Qian, X.; Liu, Y. Electrospun polyimide nanofiber-coated polyimide nonwoven fabric for hot gas filtration. *Adsorpt. Sci. Technol.* **2018**, *36*, 1734−1743.

11 Gholami, F.; Tomas, M.; Gholami, Z.; Vakili, M. Technologies for the nitrogen oxides reduction from flue gas: a review. *Sci. Total Environ.* **2020**, *714*, 136712−136737.

12 Honma, T.; Sato, T. Hydrolysis kinetics of PMDA/ODA polyimide for monomer recovery using sodium hydroxide in high-temperature water. *J. Supercrit. Fluids* **2020**, *166*, 105037.

13 Pawlowski, W. P.; Coolbaugh, D. D.; Johnson, C. J. Etch rate studies of base-catalyzed-hydrolysis of polyimide film. *J. Appl. Polym. Sci.* **1991**, *43*, 1379−1383.

14 Fang, D.; Yan, B.; Agarwal, S.; Xu, W. H.; Zhang, Q.; He, S. J.; Hou, H. Q. Electrospun poly[poly(2,5-benzophenone)]bibenzopyrrolone/ polyimide nanofiber membrane for high-temperature and strong-alkali supercapacitor. *J. Mater. Sci.* **2021**, *56*, 9344−9355.

15 Yang, K.; Ni, H. Z.; Shui, T. E.; Chi, X. Y.; Chen, W. B.; Liu, Q.; Xu, J. M.; Wang, Z. High conductivity and alkali-resistant stability of imidazole side chain crosslinked anion exchange membrane. *Polymer* **2020**, *211*, 123085−123084.

16 Tashvigh, A. A.; Feng, Y.; Weber, M.; Maletzko, C.; Chung, T. S. 110th Anniversary: selection of cross-linkers and cross-linking procedures for the fabrication of solvent-resistant nanofiltration membranes: a review. *Ind. Eng. Chem. Res* **2019**, *58*, 10678−10691.

17 See Toh, Y. H.; Lim, F. W.; Livingston, A. G. Polymeric membranes for nanofiltration in polar aprotic solvents. *J. Membr. Sci.* **2007**, *301*, 3−10.

18 Park, H. B.; Lee, C. H.; Sohn, J. Y.; Lee, Y. M.; Freeman, B. D.; Kim, H. J. Effect of crosslinked chain length in sulfonated polyimide membranes on water sorption, proton conduction, and methanol permeation properties. *J. Membr. Sci.* **2006**, *285*, 432−443.

19 Soroko, I.; Bhole, Y.; Livingston, A. G. Environmentally friendly route for the preparation of solvent resistant polyimide nanofiltration membranes. *Green Chem.* **2011**, *13*, 162−168.

20 Byun, S.; Lee, S. H.; Song, D.; Ryou, M. H.; Lee, Y. M.; Park, W. H. A crosslinked nonwoven separator based on an organosoluble polyimide for high-performance lithium-ion batteries. *J. Ind. Eng. Chem.* **2019**, *72*, 390−399.

21 Kratochvil, A. M.; Koros, W. J. Decarboxylation-induced cross-linking of a polyimide for enhanced CO_2 plasticization resistance. *Macromolecules* **2008**, *41*, 7920−7927.

22 Qiu, W.; Chen, C. C.; Xu, L.; Cui, L.; Paul, D. R.; Koros, W. J. Sub-T_g cross-linking of a polyimide membrane for enhanced CO_2 plasticization resistance for natural gas separation. *Macromolecules* **2011**, *44*, 6046−6056.

23 Zhang, C.; Li, P.; Cao, B. Decarboxylation crosslinking of polyimides with high CO_2/CH_4 separation performance and plasticization resistance. *J. Membr. Sci.* **2017**, *528*, 206−216.

24 Du, N.; Dal-Cin, M. M.; Robertson, G. P.; Guiver, M. D. Decarboxylation-induced cross-linking of polymers of intrinsic microporosity (PIMs) for membrane gas separation. *Macromolecules* **2012**, *45*, 5134−5139.

25 Cheng, Z.; Liu, Y.; Meng, C. B.; Dai, Y.; Luo, L. B.; Liu, X. Y. Constructing a weaving structure for aramid fiber by carbon nanotube-based network to simultaneously improve composites interfacial properties and compressive properties. *Compos. Sci. Technol.* **2019**, *182*, 107721−107729.

26 Zheng, S. S.; Dong, J.; Zhou, X. Y.; Li, X. T.; Zhao, X.; Zhang, Q. H. High-strength and high-modulus polyimide fibers with excellent UV and ozone resistance. *ACS Appl. Polym.* **2022**, *4*, 4558−4567.

27 Xu, Y.; Zhang, Q. Two-dimensional Fourier transform infrared (FT-IR) correlation spectroscopy study of the imidization reaction from polyamic acid to polyimide. *Appl. Spectrosc.* **2014**, *68*, 657−662.

28 Xu, S.; Wang, Y. Novel thermally cross-linked polyimide membranes for ethanol dehydration *via* pervaporation. *J. Membr. Sci.* **2015**, *496*, 142−155.

29 Xu, Y. M.; Le, N. L.; Zuo, J.; Chung, T. S. Aromatic polyimide and crosslinked thermally rearranged poly(benzoxazole-*co*-imide) membranes for isopropanol dehydration *via* pervaporation. *J. Membr. Sci.* **2016**, *499*, 317−325.

30 Fang, Y. T.; Gan, F.; Dong, J.; Zhao, X.; Li, X. T.; Zhang, Q. H. Preparation of high-performance polyimide fibers with wholly rigid structures containing benzobisoxazole moieties. *Chinese J. Polym. Sci.* **2022**, *40*, 280−289.

31 Wang, J.; Zhang, H.; Miao, Y.; Qiao, L.; Wang, X.; Wang, F. UV-curable waterborne polyurethane from CO_2-polyol with high hydrolysis resistance. *Polymer* **2016**, *100*, 219−226.

32 Fu, H.; Gong, L. B.; Gong, S. L. A new approach utilizing aza-michael addition for hydrolysis-resistance non-ionic waterborne polyester. *Polymers* **2022**, *14*, 2655−2671.

33 Yu, W.; Ko, T. M. Surface characterizations of potassium-hydroxide-modified Upilex-S® polyimide at an elevated temperature. *Eur. Polym. J.* **2001**, *37*, 1791−1799.